ISSN 2228-9860 eISSN 1906-9642 CODEN: ITJEA8

International Transaction Journal of Engineering, Management, & Applied Sciences & Technologies

http://TuEngr.com

Performance Comparison of Unsupervised Segmentation Algorithms on Rice Groundnut and Apple Plant Leaf Images

Bellapu Rajendra Prasad[1*], Tirumala Ramashri[2], Rama Naidu Kurukundu[3]

[1] *Department of Electronics & Communication Engineering, JNTUA College of Engineering, Jawaharlal Nehru Technological University Anantapur, Ananthapuramu, A.P, INDIA.*

[2] *Department of Electronics & Communication Engineering, SVU College of Engineering, Sri Venkateswara University, Tirupati, A.P, INDIA.*

**Corresponding Author (Email: rajendra.14ph0416@gmail.com).*

Paper ID: 12A12M

Volume 12 Issue 12

Received 15 July 2021
Received in revised form 10 September 2021
Accepted 22 September 2021
Available online 28 September 2021

Keywords:
Unsupervised segmentation; Graph Cut; Multi-Level Otsu; Plant Leaf Disease Detection; Semantic Segmentation; KOTSU; CHKMC; GCMO; Automatic plant disease detection; Rice image data; 2D Tsallis Entropy (2DTE); K-means Clustering (KMC); Variation of Information (VoI).

Abstract

This paper focuses on plant leaf image segmentation by considering the aspects of various unsupervised segmentation techniques for automatic plant leaf disease detection. The segmented plant leaves are crucial in automatic disease detection, quantification, and classification of plant leaf diseases. It is challenging to segment out the affected area from the images of complex backgrounds. Hence, robust semantic segmentation for automatic recognition and analysis of plant leaf disease detection is highly demanded in precision agriculture. This breakthrough is expected to demand an accurate and reliable technique for plant leaf segmentation. We propose a hybrid variant that incorporates Graph Cut (GC) and Multi-Level Otsu (MOTSU) in this paper. We compare the segmentation performance implemented on rice, groundnut, and apple plant leaf images for various unsupervised segmentation algorithms. Boundary Displacement error (BDe), Global Consistency error (GCe), Variation of Information (VoI), and Probability Rand index (PRi) are the index metrics used to evaluate the performance of the proposed model. By comparing the outcomes of the simulation, our proposed technique, Graph Cut based Multi-level Otsu (GCMO), provides better segmentation results than other existing unsupervised algorithms.

Disciplinary: Multidisciplinary (Digital Image Processing, Smart Agriculture, Machine Learning).

Cite This Article:

Prasad, B. R., Ramashri, T., Kurukundu, R. N. (2021). Performance Comparison of Unsupervised Segmentation Algorithms on Rice Groundnut and Apple Plant Leaf Images. *International Transaction Journal of Engineering, Management, & Applied Sciences & Technologies, 12*(12), 12A12M, 1-18. http://TUENGR.COM/V12/12A12M.pdf DOI: 10.14456/ITJEMAST.2021.244

1 Introduction

Segmentation techniques are classified into supervised and unsupervised segmentation techniques (Yang, et al., 2008) based on prior knowledge about the disease. Segmentation is an essential step to estimate crop loss. Rice crop occupies a prominent place in the Indian agriculture economy. Rice is cultivated in 43.86 million hectares, with 110 million metric tons yearly (AgriCoop, 2020). India plays a crucial role worldwide in producing and leading exporters of agricultural products in the future, and agriculture is the primary source of occupation; it creates employment for most people. It contributes to 18% of India's GDP.

The critical approach used in practice for diagnosing and identifying plant leaf diseases is through naked eye observation of specialists. However, the continuous supervision of experts is required to detect the diseases at their early stages. Furthermore, in some developing countries like India, farmers have to go a long way to reach experts for consultation, which is too expensive and time-consuming. Farmers are unaware of some diseases and use highly toxic chemical pesticides, which reduce the nutrients in seeds, fruits, vegetables.

According to Tropical Medicine and International Health, in A.P, an area of intensive agricultural production, southern India, the Warangal d.t records over 1000 cases of pesticide poisoning per year and hundreds of deaths (Rao, 2005). In recent years, demand has also been intensified to incorporate non-chemical approaches in managing plant leaf diseases. However, typically, non-chemical controls do not exist. So, to avoid these problems, research is undergoing for identifying the diseases in an accurate and timely way. Nowadays, deep learning models are used for disease detection in plants (Sharma et al., 2019) for minimizing crop damages, and an effective image segmentation technique is required to improve the accuracy of the deep learning models.

1.1 Image Processing Challenges

One of the critical difficulties of pre-processing plant leaf images is the non-uniformity distribution of illumination and contrast variation between foreground (FG) and background (BG) due to different lighting conditions in digital image acquisition of plant leaves. Multiple techniques have been intended to remove the backdrop in images during pre-processing. So, the exact classification of symptoms is only performed by a clear distinction between affected and healthy pixels, which is determined by the correct pre-processing step. Separating leaf elements from images that comprise different symptoms, like shape, color, texture, and most of the background areas are similar, making it difficult during segmentation and classification stages. Image segmentation techniques (Gonzalez et al., 2009) are subdivided as region growing based segmentation, threshold-based segmentation, matching segmentation, edge-based segmentation, histogram-based thresholding, Graph-based technique (Shi et al., 2000), classification-based segmentation (Tian et al., 2019). Therefore, the following are the challenge for any researcher working under machine vision applications: Accurate Detection of the diseased leaf, stem, fruit,

and quantifying the affected area of disease, to know the severity of the disease, finding the borders of the affected region, determine the features like color, shape, the texture of the affected region, determine size & shape of a leaf and classify the target correctly.

This research aims to develop a hybrid supervised segmentation technique that uses groundnut, apple, and diseased rice pictures to achieve fast and effective automatic disease detection. Most of the datasets used in this study are collected manually by visiting fields. The Ground truth images are developed by manual segmentation.

2 Image Pre-Processing

This research uses a Multi-Scale Retinex (MSR) algorithm to enhance the plant leaf image during pre-processing. Real-time images which are directly captured under sunlight are subjected to overcast or illumination problems that can be solved by the color restoration approach using relative reflectance components in the image.

Let us consider M paths to be, σ1,σ2,...,σk,...,σM starting at pixel i and ending at a random image pixel j_k, where $i_{t_k}=\sigma_k(s_k)$ and $(i_{s_k}+1)=\sigma_k(s_k+1)$ denotes the total number of pixels in the path σk and its subsequent path, respectively. Then the average relative lightness $L(i)$ of a pixel, i over all paths is defined as

$$L(i)=\frac{\sum_{i=1}^{M} L(i;j_k)}{M} \quad (1),$$

where $L(i;j_k)$ is the relative lightness of a pixel w.r.t j_k on the path σ_k

$$L(i;j_k)=\sum_{s_k=1}^{n_k}\delta\left[log\frac{I(i_{s_k})}{I(i_{s_k}+1)}\right] \quad \text{Where } \delta(T)=\begin{cases}T & if\ |T|>s\\ 0 & if\ |T|<s\end{cases} \quad (2).$$

The amount of light illuminated on an image is defined as

$$I_i(x,y)=S_i(x,y)*R_i(x,y) \quad (3),$$

$$R_i(x,y)\approx log\frac{S_i(x,y)R_i(x,y)}{\overline{S_i}\,\overline{R_i}} \quad (4).$$

The weighted sum of the output Single Scale Retinex is defined as the output of the MSR,

$$R_{MSR_i}=\sum_{n=1}^{N} w_n R_{n_i}=\sum_{n=1}^{N} w_n\left[log\, I_i(x,y)-log(F_n(x,y)*I_i(x,y))\right] \quad (5),$$

$$F_n(x,y)=C_n exp[-\frac{x^2+y^2}{2\sigma_n^2}] \quad (6).$$

3 Image Segmentation Techniques

For any segmentation technique shape of the object is one of the most significant attributes. In many computer vision tasks for an object, detection shape plays a key role rather than any other features such as image texture, boundary, and color. The ultimate goal of any image segmentation technique during the segmentation process is to segment the regions on the plant leaf image into two different classes: **Class1:** Diseased regions, where all affected pixels in the image belong to this class, and **Class2**: Healthy region, where all unaffected pixels belong to class 2. During first-level

segmentation, background removal, i.e., segmenting the plant leaf from a complex backdrop, is crucial, and it should be performed appropriately to prevent any wrong prediction. This idea has led to the development of several image segmentation techniques for segmenting diseased plant leaf images. Threshold-based (Petro et al., 2014), Colour index-based and Learning-based segmentation (Hamuda et al., 2016) are the most commonly used segmentation techniques.

3.1 Unsupervised Segmentation Techniques

Unsupervised segmentation of images remains a significant challenge and perhaps a key target for machine vision analysis. Region-based and edge-based approaches come under this category. During the first stage of segmentation, our target is to extract the leaf image from the background; hence the number of segmentations desired is two so, we set the initial N-cuts as 2. Thus, this can be achieved using a Graph Cut-based segmentation technique.

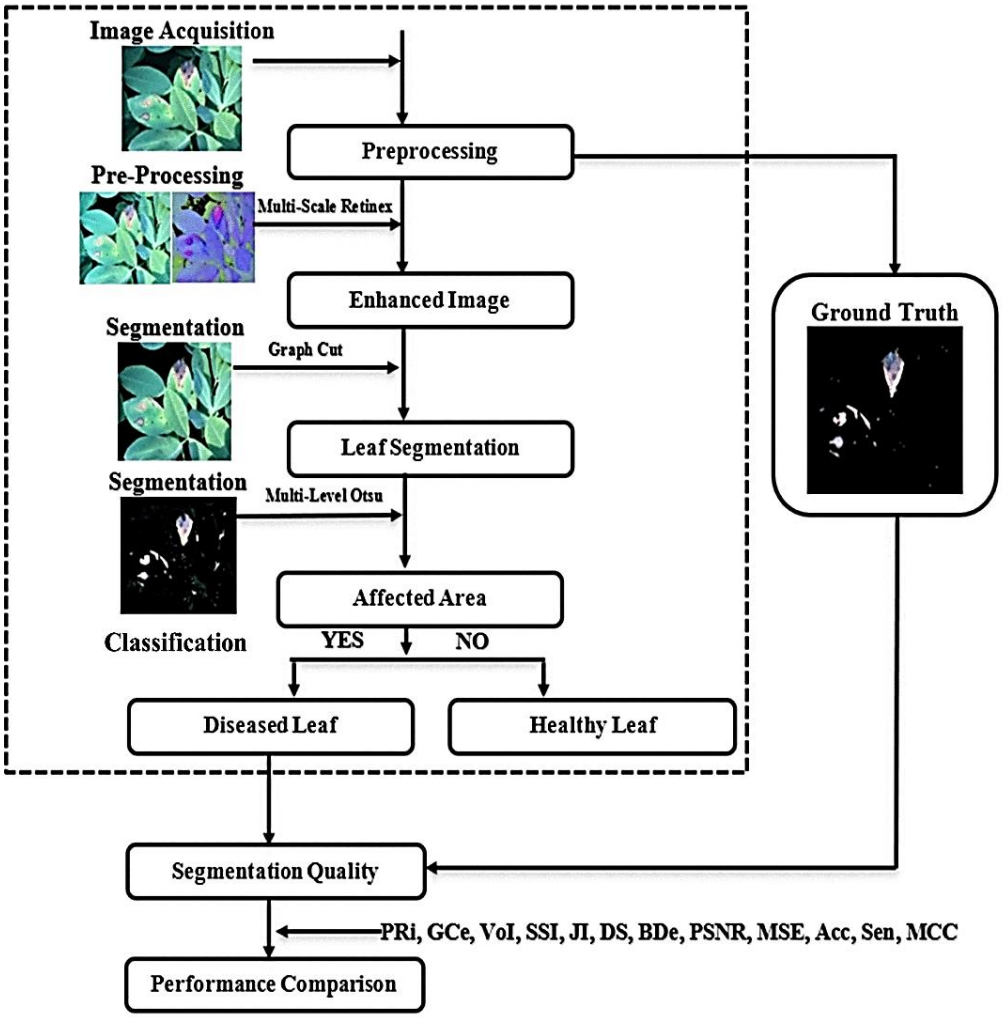

Figure 1: Block Diagram of the Proposed Model.

Next, during the second stage of segmentation, our target is to segment diseased and healthy regions to estimate the severity; hence, the cluster numbers are selected based on the segmentation preview shown by MATLAB to obtain accurate segmentation for different images. We choose four different clusters K=6,7,8,9 for all the images and finally select one K value by

comparing four segmentation outputs for each K value depending on the image. This process is followed by all the techniques used in this work.

3.1.1 Segmentation using K-means Clustering (KMC)

Cluster-based segmentation is an example of an unsupervised segmentation strategy that segments identical patterns into clusters. Some of the famous and well-developed techniques used for segmentation are clustering techniques (Tian, K., Li et al., 2019): K-means clustering method, partitions image pixels into K number of mutually exclusive regions or clusters and returns the class of the cluster based on centroid or center, distance metric such as Squared Euclidean, Cityblock, Hamming, Cosine distance measures respectively

$$d(p, c) = (p, c)\ (p, c)' \quad (7),$$

$$d(p, c) = \sum_{i=1}^{n} |p_i - c_i| \quad (8)$$

$$d(p, c) = \frac{1}{p} \sum M(x_j \neq y_j) \quad (9)$$

$$d(p, c) = 1 - \frac{pc'}{\sqrt{(pp')(cc')}} \quad (10)$$

3.1.2 Colour Histogram-based Segmentation using K-means Clustering (CHKMC)

This technique groups pixels into K groups based on color similarity (Zhang et al., 2004). Color similarity is estimated based on selected color space.

Algorithm: Colour Histogram-based Plant Leaf image Segmentation using K-means Clustering.

1: Randomly initialize the number of clusters C1, C2,...., CK, and cluster centers using selected geometric color Space.

2: Estimates the color peaks using histogram thresholding.

3: For the given cluster centers, calculate Euclidean distance for each color pixel P and assign the min distance pixel to the cluster Ck.

$$C_k = arg\ min\ \|x_i - \mu_k\|^2 \quad (11),$$

C_k represents K^{th} distance pixel, x_i = i^{th} Colour pixel, and μ_k = k^{th} Cluster center.

4: Repeat steps 2 and 3 until all pixels are assigned to any one of the clusters.

3.1.3 K-Means and Otsu's based Plant Leaf Image Segmentation (KOTSU)

The Otsu thresholding technique is named after its inventor Nobuyuki Otsu; the Otsu threshold technique performs segmentation by computing the optimal threshold (Yue et al., 2019) value on an image histogram. It segments the images by computing within-class variance or between-class variance.

$$\sigma^2 = \frac{\sum_{i=0}^{N} (x_i - \mu)^2}{N} \quad (12).$$

Weighted minimized variance is defined as

$$\sigma_w^2(t) = w_1(t) * \sigma_1^2(t) + w_2(t) * \sigma_2^2(t) \quad (13),$$

$$\sigma_b^2(t) = w_1(t) * w_2(t) [\mu_1(t) - \mu_2(t)]^2 \quad (14),$$

$$w_1(t) = \sum_{i=1}^{t} p(i) \ , \ w_2(t) = \sum_{i=t+1}^{L-1} p(i) \quad (15).$$

Therefore, the pixel intensity values of cluster C_1 are i=1 to i=t, and C_2 are i=t+1 to i=I, where 'L' represents maximum intensity value. Then obtain the means for clusters C_1 and C_2

$$\mu_1(t) = \sum_{i=1}^{t} \frac{i*p(i)}{w_1(t)} \quad (16),$$

$$\mu_2(t) = \sum_{i=t+1}^{L-1} \frac{i*p(i)}{w_2(t)} \quad (17).$$

3.1.4 Plant Leaf Image Segmentation using Multi-Level Otsu's Thresholding

In this technique, images are segmented into distinct regions by using different threshold level values. The histograms of such multiple background images contain multiple valleys hence called multimodal histograms. This histogram is successful and accurate only when there is a clear distinction between FG and BG objects. Figure 2 shows Multimodal histogram segmentation.

3.1.5 Plant Leaf Image Segmentation based on Entropy-Based Thresholding

Bilevel thresholding extensively uses entropy-based thresholding. It uses the measure of information in an image defined by Shannon (Zhou et al., 2014). Threshold value plays a vital role in the effectual image segmentation; therefore, variants of Shannon's entropy are used to select optimal threshold values, which are used for segmenting the FG and BG. Entropy can be calculated by using 1. Kapur's entropy: The computation of FG and BG segment entropies using Kapur's entropy thresholding technique using Equation (18).

$$H_{fg}(t) - \sum_{G=0}^{t} \frac{p(G)}{p_{fg}(t)} ln \frac{p(G)}{p_{fg}(t)} \quad (18).$$

$$H_{bg}(t) - \sum_{G=t+1}^{L} \frac{p(G)}{p_{bg}(t)} ln \frac{p(G)}{p_{bg}(t)} \quad (19).$$

$$p(G) = \frac{h(G)}{N}, \text{ G = 0,1,2,..., L-1} \quad (20).$$

2. Renyie's entropy: The computation of FG and BG segment entropies using Renyi's entropy thresholding technique.

$$H_{fg} = \frac{1}{1-\rho} ln \left[\sum_{G=0}^{t} \left(\frac{p(G)}{p_{fg}(t)} \right)^{\sigma} \right] \quad (21),$$

$$H_{bg} = \frac{1}{1-\rho} ln \left[\sum_{G=t+1}^{L-1} \left(\frac{p(G)}{p_{bg}(t)} \right)^{\sigma} \right] \quad (22).$$

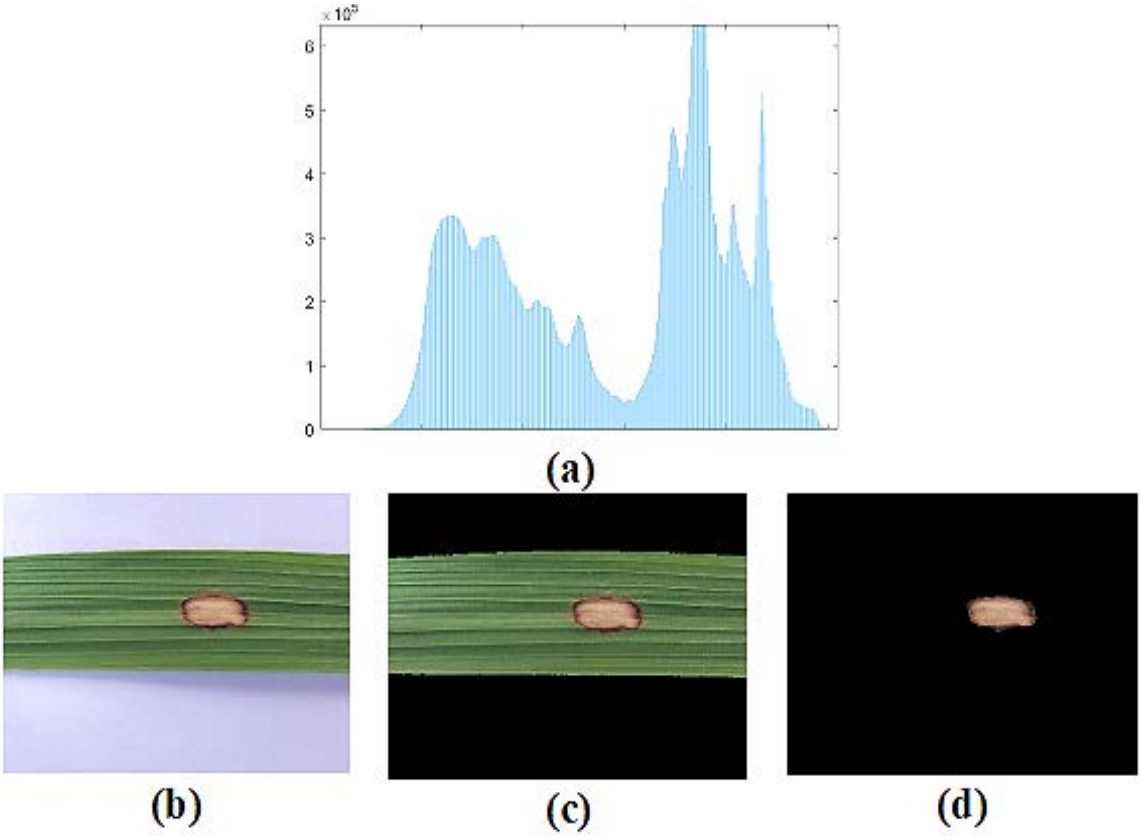

Figure 2: Multi-level Image Thresholding: (a) Multimodal Histogram of Input Image, (b) Input Leaf Image, (c) FG Segmentation, (d) Disease Segmentation

3.1.6 Plant Leaf Image Segmentation based on 2D Tsallis Entropy (2DTE)

The plant leaf image consists of two independent parts: FG object set F and BG objects set B. The interrelation between these sets using 2D Tsallis entropy (Naidu et al., 2017) is defined as

$$S_q(F) = \frac{1-\sum_{i=0}^{t} \sum_{j=0}^{s} \left(\frac{p(i,j)}{p_A(t,s)}\right)^q}{q-1} \quad (23),$$

$$S_q(B) = \frac{1-\sum_{i=t+1}^{255} \sum_{j=s+1}^{255} \left(\frac{p(i,j)}{p_B(t,s)}\right)^q}{q-1} \quad (24),$$

where $P_A(t,s)$ and $P_B(t,s)$ are posterior class probabilities of FG and BG independently distributed objects defined by

$$p_A(t,s) = \sum_{i=0}^{t} \sum_{j=0}^{s} p(i,j) \quad (25),$$

$$p_B(t,s) = \sum_{i=t+1}^{255} \sum_{j=s+1}^{255} p(i,j) \quad (26).$$

The definition of 2D Tsallis-Havrda-Charvat entropy (Borjigin et al., 2019) of the whole digital image is defined by

$$S_q(t,s) = S_q(FG) + S_q(BG) + (1-q)\, S_q(FG) S_q(BG) \quad (27),$$

$$(t*, s*) = \text{Argmax } Sq(t,s) \quad (28).$$

Plant Leaf Image Segmentation based on Graph Cut Based Multilevel Otsu (GCMO) Technique

A hybrid technique is proposed for plant leaf image segmentation for both complex and simple background images. Graph cut-based segmentation employs both boundary and regional information for segmentation; hence it achieves optimal results for separating BG and FG information in an image by splitting the graph into several sub-graphs such that each graph has a relevant object of interest in the image. Graph cut algorithm (Chen et al., 2011) cuts the image regions first by grouping the regions using perspectival grouping laws like similarity and continuity (Liu et al., 2011), and then cut the regions by calculating the dissimilarity degree between the regions. The block diagram of the proposed model is shown in Figure 1.

For a given Graph set $G = \{N, E\}$, where $N = \{n_1, n_2, .., n_n\}$ is nodes set or vertices set corresponding to image elements in the Euclidian space. Edge E is known as the set of edges connecting a pair of nodes. The weight vector W(i,j) measures the similarity based on the certain property between the two nodes connected at each edge (i,j). The dissimilarity degree can be calculated as the cumulative weight of the edges removed from these sets (Doggaz et al., 2011). As a result, an image's segmentation can be viewed as a graph cut and is defined as

$$cut(A, B) = \sum_{i \in A,\ j \in B} w(i, j) \quad (29).$$

Algorithm: Plant Leaf Image Segmentation Based on a Hybrid GCMO Technique.

Step 1: Map all the image elements to a graph where pixel regions or user-drawn markers can be the nodes.

Step 2: From a graph structure with a set of boundaries or edges(E) (the connection between pairs of nodes) and a set of nodes (N) (vertices) and, and estimate the similarity matrix S.

$G=\{N, E\}$ and $S = [S_{ij}]$

Step 3: Compute the degree of node d_i and volume of set vol(A).

$d_i = \Sigma_j S_{ij}$ and $Vol(A) = \Sigma_{i \in A} d_i$ $A \subseteq V$

Step 4: Cut the graph using Equation (29).

Step 5: Compute the Multi-level Otsu technique to the output of step 4.

3.2 Quantitative Performance Indices

Let image contains the N number of pixels. X= {0,1,2,...,N} with (0 to L-1) intensity values. Considering the clusters $C_1=\{P_1, P_2, .., P_k\}$ be from ground truth image and $C_2 = \{P'_1, P'_2, ..., P'_k\}$ be from a segmented image, List of performance indexes.

Probability Rand index (PRi) : $PRi = \begin{cases} 0, when\ C1 \neq C2 \\ 1, when\ C1 = C2 \end{cases}$

Global Consistency error (GCe) : $GCe(C_1, C_2) = \frac{1}{n} min(\sum_i E(C_1, C_2, p_i), \sum_i E(C_2, C_1, p_i))$

Where $E(C_1, C_2, p_i) = \frac{|R(C_1, p_i) - R(C_2, p_i)|}{|R(C_1, p_i)|}$

Peak Signal to Noise Ratio (PSNR) : $PSNR = 10 * log_{10} \frac{(255)^2}{MSE}$

Mean Square Error (MSE) : $$MSE = \frac{1}{MN}\sum_{s=1}^{m}\sum_{t=1}^{n}(H-G)^2$$

Variation of Information (VoI) : $$M_i(C_1,C_2) = \sum_{i=1}^{k}\sum_{i'=1}^{k'} P(C_1,C_2)log\frac{P(C_1,C_2)}{P(C_1)\,P(C_2)}$$

Boundary Displacement error (BDe) : $$BDe(s,t) = \begin{cases}\dfrac{s-t}{L-1} & where\ 0<(s-t)\end{cases}$$

Structural Similarity Index (SSI) : $$SSIM(H,G) = \frac{(2\mu_H\mu_G + k_1)(2\sigma_{HG} + k_2)}{(\mu_H^2\mu_G^2 + k_1)(\sigma_H^2\sigma_G^2 + k_2)}$$

Jaccard Index (JI) : $$JI = \frac{|H \cap G|}{|H \cup G|} = \frac{|H \cap G|}{|H| + |G| - |H \cap G|}$$

Dice Similarity (DS) : $$D = 2\frac{|H \cap G|}{|H \cup G|}$$

Accuracy (Acc) : $$Acc = \frac{(T_p) + (T_n)}{(T_p) + (T_n) + (F_p) + (F_n)}$$

Sensitivity (Sen) : $$Sen = \frac{T_p}{T_p + F_n}$$

Matthews Correlation Coefficient (MCC) : $$MCC = \frac{(T_p \times T_n) - (F_p \times F_n)}{\left(\sqrt{(T_p + F_n)(TP + F_p)(T_n + F_n)(T_n + F_p)}\right)} \times 100$$

4 Results and Discussion

The proposed work was carried out on MATLAB R2019a version software with a 2.20GHz Intel core 64-bit i7 processor with 8GB RAM installed on windows 10 laptop. All the images used in this work shown in Figure 3 are enhanced using the MSR algorithm during pre-processing to evaluate the proposed segmentation algorithm's performance. The results show that this enhancement approach provides the best color restoration by preserving subtle details of images like edges and boundaries, enhancing image details, restoring color, and improving contrast. This procedure is followed to obtain the best comparison. The quantitative analysis (Huang, Q et al., 1995) of K-means-based Otsu thresholding (Zhou et al., 2013) (KOTSU), Colour histogram-based segmentation using K-means clustering (Shen et al., 2016) **(**CHKMC), 2D Tsallis Entropy **(**2DTE), and proposed Graph cut Based multi-level Otsu **(**GCMO) are discussed in this section.

The segmentation results and evaluation metrics for plant diseased leaf images are shown in Tables 1-4. The rice image data set used in this work is collected from the Agriculture Research Station (ARS), Nellore, A.P, and groundnut images from the Regional Agricultural Research Station (RARS), Tirupati, A.P, India.

To measure the performance of the proposed method, the apple plant data set is taken from the plant Village website, which is accessible online, along with ground truth images. Even though we considered 12 evolution performance comparison metrics in this paper, to avoid confusion in plots, we plot only the comparison of PSNR and accuracy in the right-side plot and PRi, VoI, and SSI on the left side plot for segmentation techniques performed plant diseased images with Simple and complex backgrounds in Figures 6-9.

Figure 3 shows the raw data set containing 15 sample leaf images from the total dataset of rice, groundnut, and apple plants used for pre-processing and further for segmentation and comparison. 1a, 2a, 3a, 4a, and 5a images are ground truth images of the segmented leaf, 1b, 2b, 3b, 4b, and 5b images are ground truth images of the region of interest (ROI) for disease classification, i.e., diseases segmented regions, and 1c, 2c, 3c, 4c, and 5c images are ground truth mask of the segmented leaf. 1d, 2d, 3d, 4d, and 5d images in Figures 4 and 5 show the visual results of the KOTSU technique. 1e, 2e, 3e, 4e, and 5e images in Figures 4 and 5 show the visual results of CHKMC. 1f, 2f, 3f, 4f, and 5f images show the visual results of 2DTE. 1g, 2g, 3g, 4g, and 5g images show the visual results of the proposed GCMO technique. From Figures 4 and 5, it is evident that GCMO achieves the best discrimination between ROI, BG, and FG.

The results illustrated in Table.1 show that the proposed GCMO technique's accuracy achieves 98.42% for RSI_1 and 90.09% for $RSI_{2,}$ which is slightly near to KOTSU and 2DTE. Segmentation accuracy, BDE, and JI are low for CHKMC. Overall, CHKMC fails to achieve the best performance in all the evaluation metrics. Whereas 2DTE has the best VoI when compared to the remaining techniques. JI, DS, PRi, GCe, BDe, and MCC are best for GCMO for both RS_1 and RS_2 images, which decides the quality and accuracy of the segmentation technique, which is graphically illustrated in Figure 6.

Table 2 summarizes the segmentation performance on rice plant leaf diseased images with complex backgrounds. It shows that CHKMC shows an abysmal performance of accuracy of 15.421% and 51.75% on plant leaf images of complex background RCI_1 and RCI_3, respectively. So, it is evident that CHKMC is very sensitive to images of complex backgrounds. Table 4 shows that the proposed GCMO technique's accuracy achieves 96.525% for GSI_1 and 97.176% for $AI_{1,}$ which is slightly near to KOTSU and 2DTE.

Table 1: Performance Comparison of Segmentation techniques on Rice Plant Leaf Diseased Images with Simple Background.

Metrics	Segmentation Techniques							
	KOTSU		CHKMC		2DTE		GCMO	
	RSI1	RSI2	RSI1	RSI2	RSI1	RSI2	RSI1	RSI2
PRi	0.95	0.77	0.58	0.65	0.95	0.82	0.96	0.82
GCe	0.013	0.017	0.018	0.018	0.012	0.017	0.012	0.017
PSNR	25.76	17.11	21.37	19.57	28.30	20.47	29.30	21.57
MSE	27.12	47.61	30.03	23.55	22.56	18.19	23.46	19.29
VoI	0.178	0.607	0.926	0.827	0.131	0.412	0.141	0.512
BDe	37.93	12.69	66.91	11.51	10.76	8.253	11.75	9.263
SSI	0.99	0.98	0.96	0.97	0.89	0.89	0.99	0.98
JI	30.72	6.727	3.194	3.909	36.77	7.64	37.78	8.634
DS	47.01	12.60	6.19	7.525	52.82	14.88	54.84	15.89
Acc	97.83	86.94	70.91	77.40	97.12	89.08	98.42	90.09
MCC	54.82	24.14	15.02	17.03	59.98	26.66	60.97	27.76
Sen	30.72	6.27	3.193	3.91	35.77	7.65	37.78	8.639

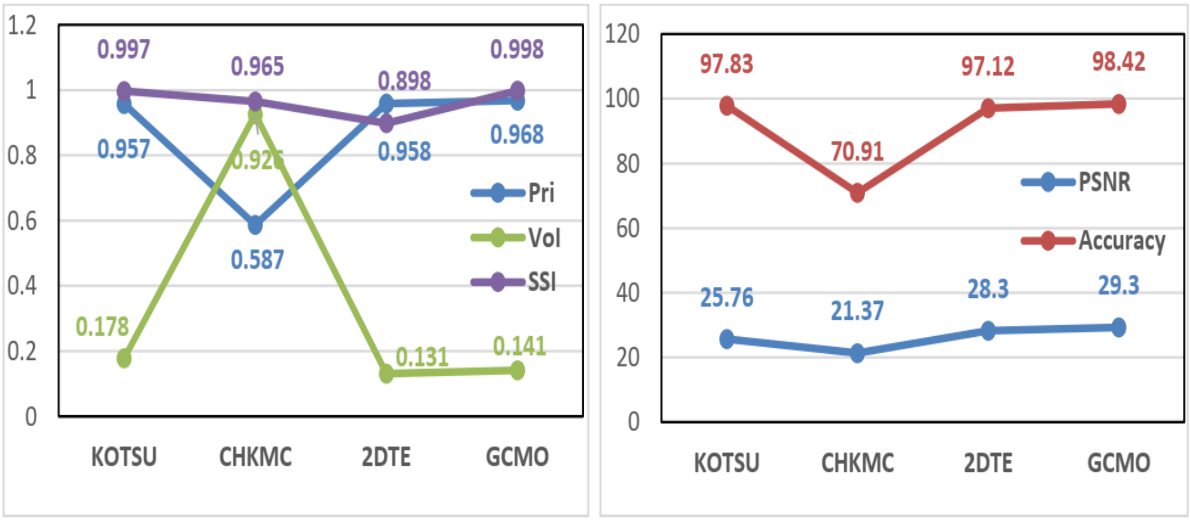

Figure 6: Graphical comparison of proposed GCMO technique with existing techniques considering rice plant leaf diseased image with a simple background (RSI_1).

In contrast, CHKMC has shown low performance. Tp=3299, Tn=204482, Fp=768, and Fn=53595 are predicted values of the CHKMC technique therefore, the misclassification rate is 20.73%, which is high compared to other techniques.

Table 2: Performance Comparison of Segmentation techniques on Rice Plant Leaf Diseased Images with Complex Background.

Segmentation Techniques								
Metrics	KOTSU		CHKMC		2DTE		GCMO	
	RCI1	RCI3	RCI1	RCI3	RCI1	RCI3	RCI1	RCI3
PRi	0.524	0.668	0.739	0.5006	0.761	0.568	0.957	0.957
GCe	0.011	0.008	0.011	0.008	0.011	0.007	0.009	0.007
PSNR	22.91	24.00	13.32	10.56	14.31	24.12	27.41	27.03
MSE	24.39	19.78	40.42	67.24	34.00	19.68	20.80	16.39
VoI	1.005	0.771	0.654	1.036	0.613	0.871	0.173	0.170
BDe	76.056	59.212	41.372	61.586	32.510	58.222	32.170	18.88
SSI	0.952	0.975	0.888	0.940	0.887	0.878	0.997	0.997
JI	1.426	2.032	0.671	0.787	0.659	2.133	20.442	15.772
DS	2.812	3.983	1.335	1.562	1.311	3.893	33.945	27.247
Acc	61.009	79.02	15.421	51.75	13.863	78.12	70.818	83.851
MCC	9.162	12.565	3.167	5.120	2.970	12.655	44.337	37.779
Sen	1.426	2.032	0.671	0.788	0.659	2.302	20.528	16.007

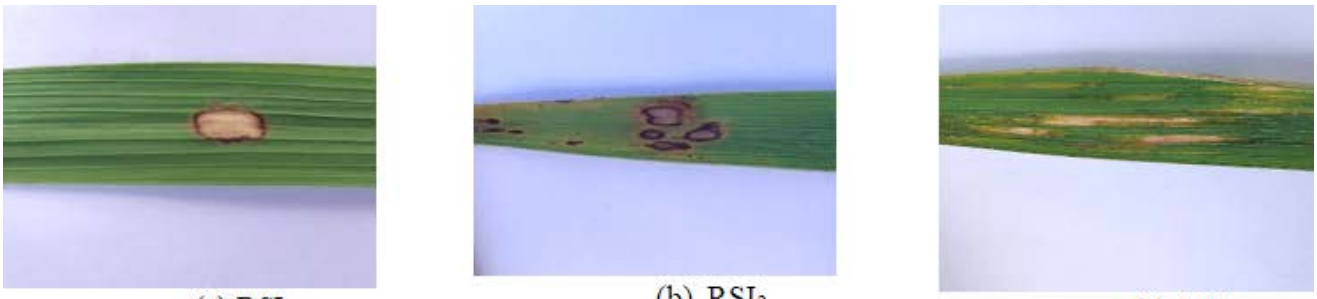

(a) RSI_1 (b) RSI_2 (c) RSI_3

$RSI_{1,2,3}$ = Rice Leaf Image 1,2,3 with Simple background
(1. Brown Spot 2. Wheat Rust 3. Early Leaf Spot)

(d) RCI_1 (e) RCI_2 (f) RCI_3

$RCI_{1,2,3}$ = Rice Leaf Image 1,2,3 with Complex background
(1.Red Rot, 2.Leaf Blast, 3.Bacterial Leaf Streak)

(g) GCI_1 (h) GCI_2 (i) GCI_3

$GCI_{1,2,3}$ = Groundnut Leaf Image 1,2,3 with Complex bakground
(1.Alternaria Leaf Sopt 2.Leaf Scorch 3. Phyllostica Leaf Spot)

(j) GSI_1 (k) GSI_2 (l) GSI_3

$GSI_{1,2,3}$ = Groundnut Leaf Image 1,2,3 with Simple bakground
(1.Alternaria Leaf Sopt 2.Leaf Scorch 3. Phyllostica Leaf Spot)

(m) AI_1 (n) AI_2 (o) AI_3

$AI_{1,2,3}$ = Apple Leaf Image 1,2,3 (1.Black Rot, 2.Cedar rust, 3.Apple scab)

Figure 3: Rice, Groundnut, and Apple image dataset with simple and complex backgrounds

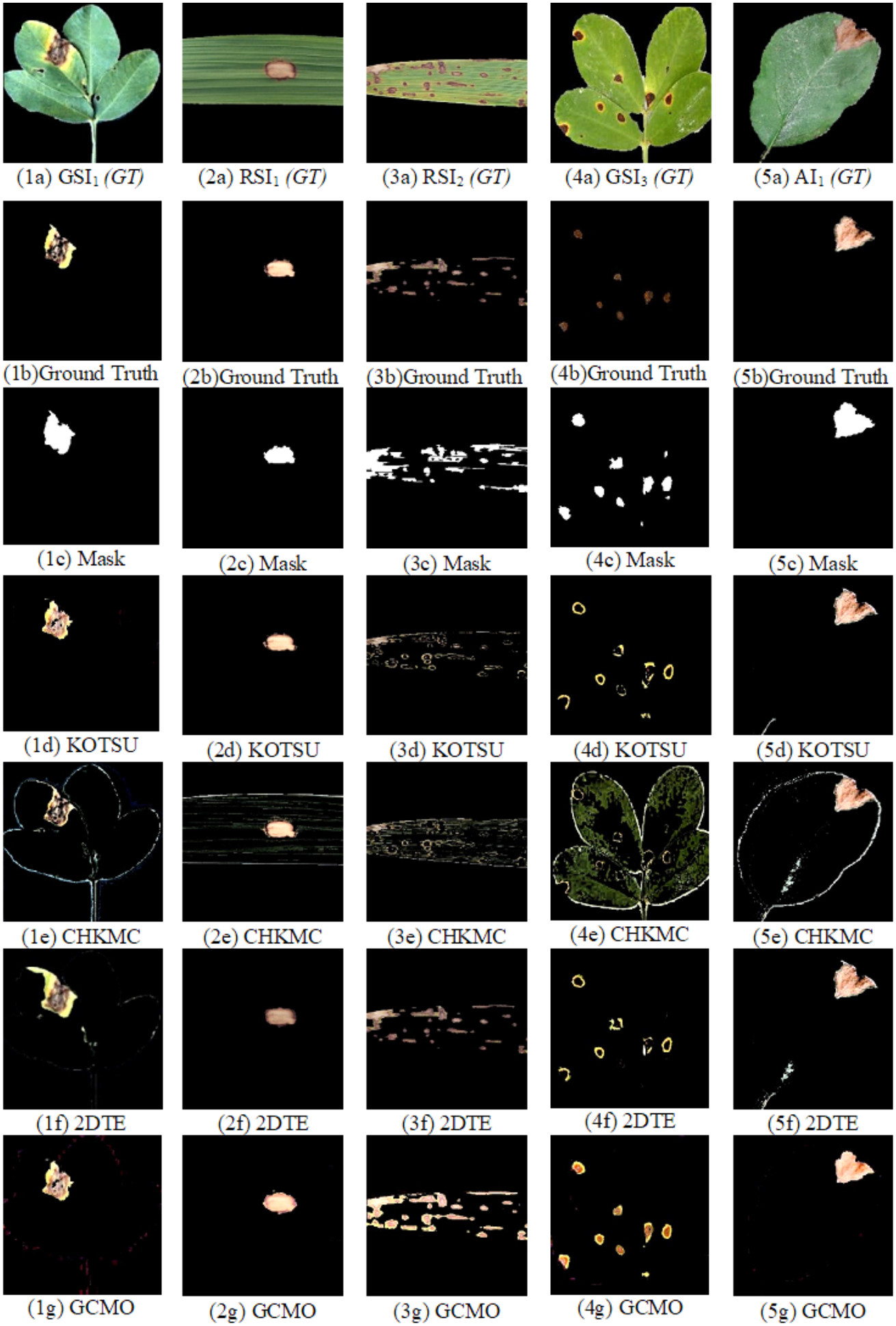

Figure 4: Segmentation results of various techniques on Groundnut, Rice, and Apple plant Leaf Diseased Images with Simple background.

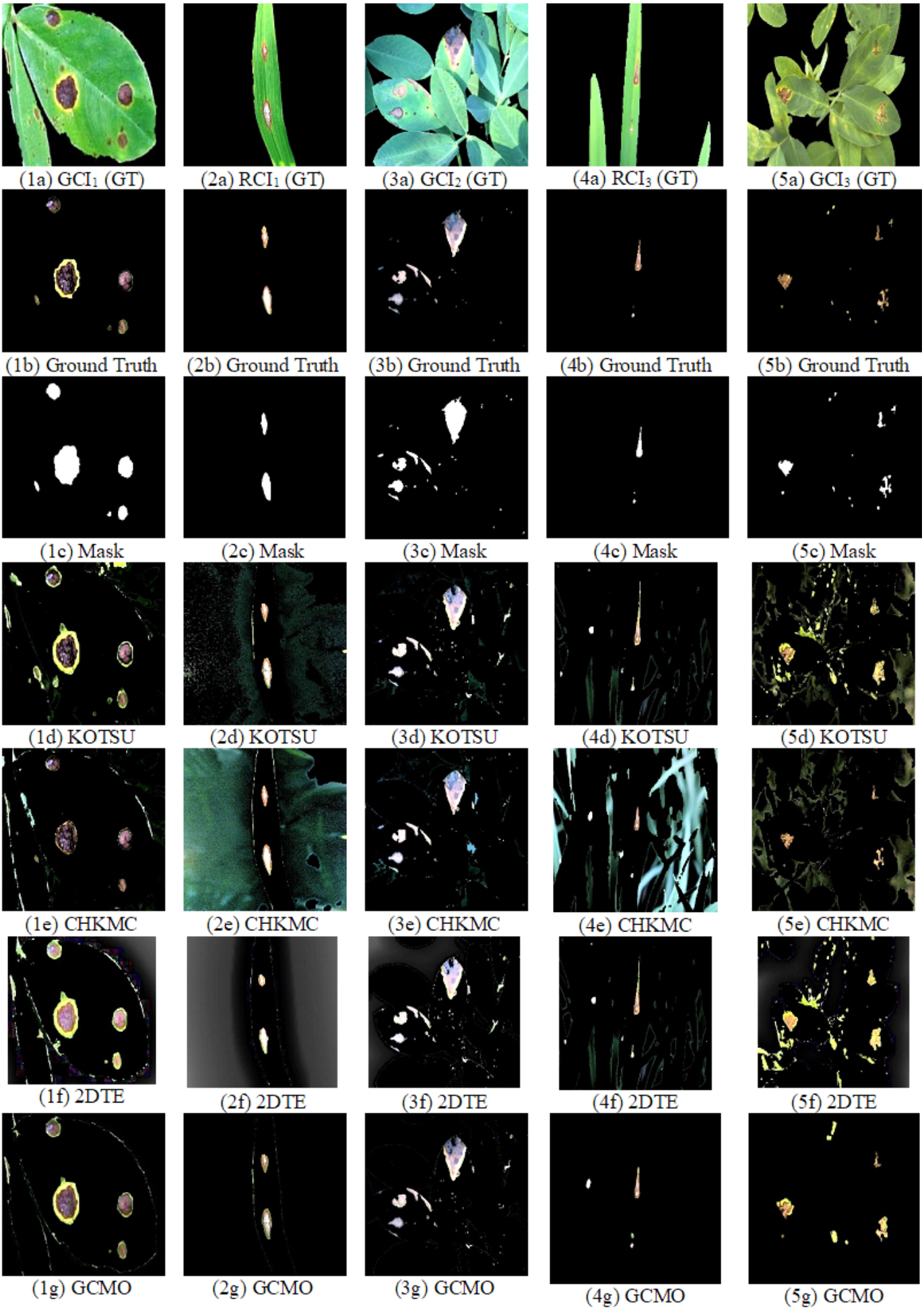

Figure 5: Segmentation Results of various techniques on Groundnut, Rice, and Apple plant Leaf Diseased Images with Complex background.

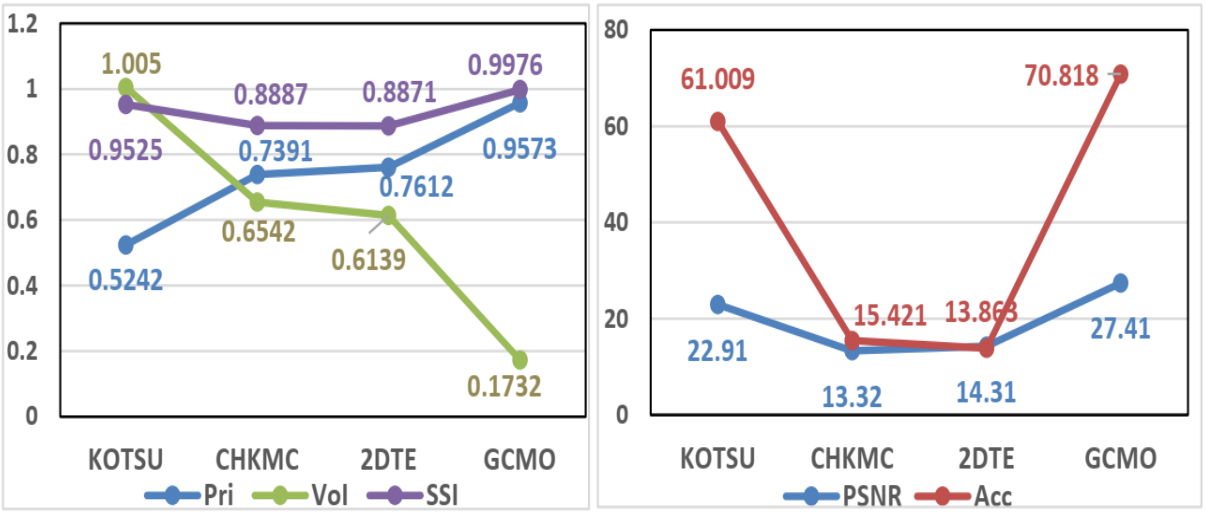

Figure 7: Graphical comparison of proposed GCMO technique with existing techniques considering rice plant leaf diseased image with a complex background (RCI1).

Table 3: Performance Comparison of Segmentation techniques on Groundnut Plant Leaf Diseased Images with Complex Background.

Metrics	Segmentation Techniques							
	KOTSU		CHKMC		2DTE		GCMO	
	GCI_1	GCI_2	GCI_1	GCI_2	GCI_1	GCI_2	GCI_1	GCI_2
PRi	0.630	0.657	0.647	0.666	0.509	0.594	0.707	0.769
GCe	0.026	0.046	0.027	0.045	0.027	0.047	0.026	0.043
PSNR	18.14	20.93	17.87	22.31	15.36	21.40	19.01	21.38
MSE	39.71	41.70	30.60	38.97	49.54	40.57	37.69	41.26
VoI	0.875	0.870	0.868	0.858	1.065	0.979	0.744	0.664
BDe	49.3	34.76	48.68	35.66	41.38	32.83	44.57	32.89
SSI	0.971	0.975	0.973	0.976	0.945	0.966	0.979	0.986
JI	5.417	10.42	4.536	10.65	3.147	8.204	7.302	16.08
DS	10.27	18.88	8.679	19.25	6.102	15.16	13.61	27.70
Acc	75.52	78.06	77.17	78.83	56.98	71.7	82.20	86.68
MCC	20.18	28.32	15.10	28.54	13.27	23.84	24.46	37.15
Sen	5.417	10.42	4.597	10.67	3.147	8.214	7.302	16.09

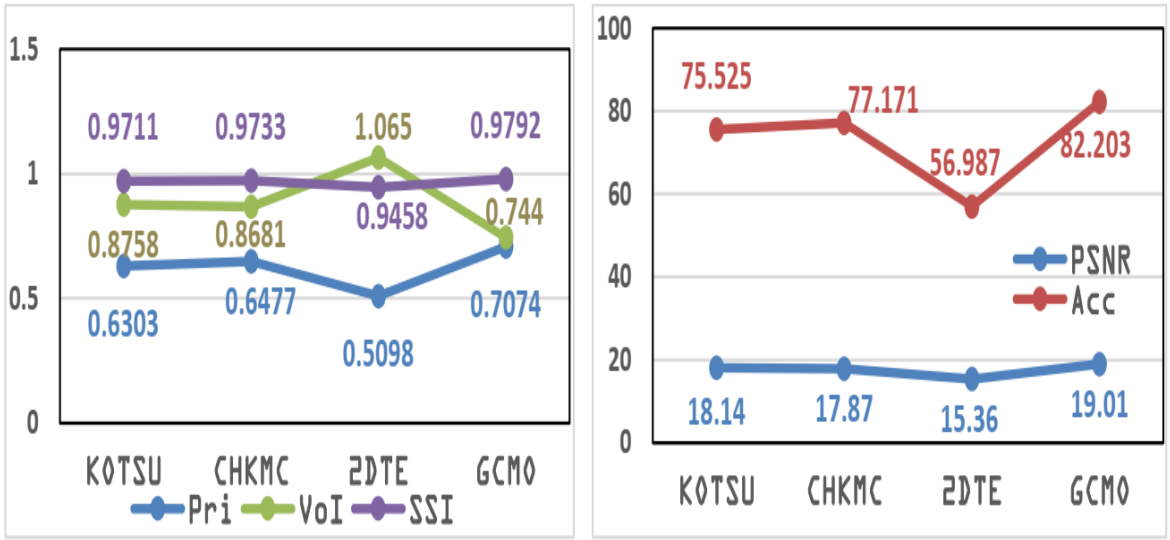

Figure 8: Graphical comparison of proposed GCMO technique with existing techniques considering groundnut plant leaf diseased image with a complex background (GCI1).

Table 4: Performance Comparison of Segmentation techniques on Groundnut and Apple Plant Leaf Disease Images with Simple Background

Metrics	Segmentation Techniques							
	KOTSU		CHKMC		2DTE		GCMO	
	GSI_1	AI_1	GSI_1	AI_1	GSI_1	AI_1	GSI_1	AI_1
PRi	0.82	0.93	0.67	0.77	0.83	0.91	0.93	0.94
GCe	0.027	0.024	0.029	0.032	0.027	0.026	0.022	0.022
PSNR	22.83	25.23	18.60	17.97	22.65	22.95	22.91	26.41
MSE	29.16	31.59	31.65	42.04	28.06	33.52	27.80	30.86
VoI	0.52	0.27	0.83	0.62	0.51	0.32	0.27	0.23
BDe	82.07	109.2	76.98	115.	82.34	109.8	49.78	72.26
SSI	0.98	0.99	0.97	0.98	0.99	0.99	0.99	0.99
JI	13.40	33.93	5.72	12.5	13.74	28.01	29.72	39.23
DS	23.64	50.67	10.82	22.2	24.17	43.76	45.82	56.36
Acc	90.49	96.43	79.26	87.2	90.87	95.29	96.52	97.17
MCC	33.82	57.16	18.09	33.0	34.11	51.62	52.44	61.61
Sen	13.50	33.94	5.79	12.5	13.87	28.01	30.22	39.32

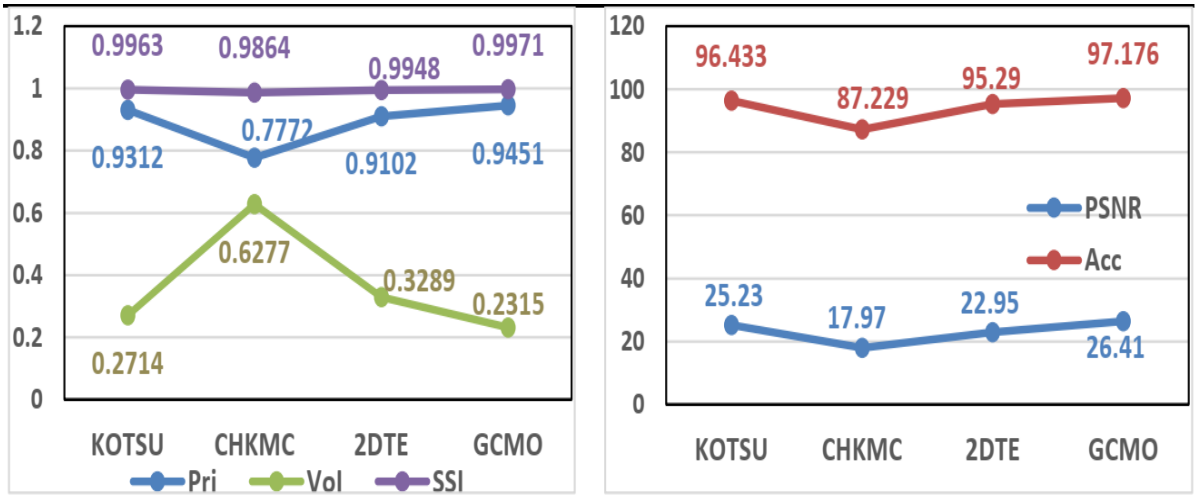

Figure 9: Graphical comparison of proposed GCMO technique with existing techniques considering apple plant leaf diseased image with simple background (AI1).

5 Conclusion

This research aimed to investigate and assess Unsupervised approaches of segmentation on plant leaf disease. We have compared the quantitative and visual results of the proposed GCMO with the remaining three approaches to support our process. We have also shown that GCMO not only produces decent results on standard test datasets collected from the plant village website but also on the real-time dataset, which we manually collected from fields. From the results formulated in Tables 1-4, it is evident that KOTSU is closer to the proposed GCMO for the images of a kind simple background, but for images of the complex background, the proposed GCMO is far superior to other techniques, which has potential for accurate segmentation. The method adopted is invariant to uneven light and noise conditions, which occurs in real-time images captured outdoor. From these results, it is clear that unsupervised segmentation techniques give the best support to improve the accuracy of various recognition algorithms. Thus, we can conclude that our proposed GCMO technique is a reliable and effective image segmentation model for plant leaf disease detection and further can be applied to other segmentation problems.

As a future extension of our work, it may be helpful to develop a segmentation model that combines the segmented features data to train the model. It will be an essential move towards the supervised segmentation of images.

6 Availability of Data and Material

All Information is included in the work and is available upon request to the corresponding author.

7 References

AgriCoop. (2020). *Annual report*. Department of Agriculture Cooperation & Farmers Welfare. https://agricoop.nic.in/annual-report

Arora, S., Acharya, J., Verma, A., & Panigrahi, P. K. (2008). Multilevel thresholding for image segmentation through a fast statistical recursive algorithm. *Pattern Recognition Letters, 29*(2), 119-125. DOI: 10.1016/j.patrec.2007.09.005

Belgiu, M., & Drăguţ, L. (2014). Comparing supervised and unsupervised multiresolution segmentation approaches for extracting buildings from very high-resolution imagery. *ISPRS Journal of Photogrammetry and Remote Sensing*, 96, 67-75. DOI: 10.1016/j.isprsjprs.2014.07.002

Borjigin, S., & Sahoo, P. K. (2019). Color image segmentation based on multi-level Tsallis-Havrda-Charvát entropy and 2D histogram using PSO algorithms. *Pattern Recognition*, 92, 107-118. DOI: 10.1016/j.patcog.2019.03.011

Chen, X., & Pan, L. (2018). A survey of graph cuts/graph search-based medical image segmentation. *IEEE reviews in biomedical engineering*, *11*, 112-124.

Dev, S., Lee, Y. & Winkler, S., (2017). Color-Based Segmentation of Sky/Cloud Images from Ground-Based Cameras. *IEEE Journal of Selected Topics in Applied Earth Observations and Remote Sensing*, 10(1), 231-242.

Doggaz, N., & Ferjani, I. (2011, September). Image segmentation using normalized cuts and efficient graph-based segmentation. In *International Conference on Image Analysis and Processing* (pp. 229-240). Springer, Berlin, Heidelberg.

Gonzalez, R. C., Woods, R. E., & Masters, B. R. (2009). *Digital Image Processing*. Third Ed.

Hedar, A. R., Ibrahim, A. M. M., & Sewisy, A. A. (2018). K-means cloning: adaptive spherical k-means clustering. *Algorithms, 11*(10), 151.

Liu, J., & Wang, H.-. (2011). A Graph Cuts Based Interactive Image Segmentation Method. *Journal of Electronics & Information Technology, 30*(8), 1973-1976. DOI: 10.3724/sp.j.1146.2007.00075

Mason, J. B., Sanders, D., & Galloway, R. (2006). *Community health and nutrition programs. In Disease Control Priorities in Developing Countries*. 2nd Ed., The International Bank for Reconstruction and Development/The World Bank. DOI: 10.1016/j.jmwh.2007.03.026

Naidu M.S.R., & Rajesh Kumar P. (2017) Tsallis Entropy Based Image Thresholding for Image Segmentation. In: Behera H., Mohapatra D. (eds) Computational Intelligence in Data Mining. Advances in Intelligent Systems and Computing, Springer, Singapore. vol 556.

Petro, A., Sbert, C. & Morel, J. (2014). Multiscale Retinex. *Image Processing on Line*, 4, pp.71-88. DOI: 10.5201/ipol.2014.107

Rao, C. S., Venkateswarlu, V., Surender, T., & Buckley, N., (2005). Pesticide poisoning in south India: opportunities for prevention and improved medical management. *Tropical Medicine and International Health*, 10(6), pp.581-588. DOI: 10.1111/j.1365-3156.2005.01412.x

Sharma, P., Berwal, Y. P. S., & Ghai, W. (2019). Performance analysis of deep learning CNN models for disease detection in plants using image segmentation. *Information Processing in Agriculture*. DOI: 10.1016/j.inpa.2019.11.001

Shen, J., Hao, X., Liang, Z., Liu, Y., & Shao, L. (2016). Real-Time Superpixel Segmentation by DBSCAN Clustering Algorithm. *IEEE Transactions on Image Processing, 25*(12), 5933-5942.

Shi, J., & Malik, J. (2000). Normalized cuts and image segmentation. *IEEE Transactions on pattern analysis and machine intelligence*, *22*(8), 888-905. DOI: 10.1109/34.868688

Tian, K., Li, J., Zeng, J., & Zhang, L. (2019). Segmentation of tomato leaf images based on adaptive clustering number of K-means algorithm. *Computers and Electronics in Agriculture*, 165, p.104962. DOI: 10.1016/j.compag.2019.104962

Yang, A. Y., Wright, J., & Sastry, S. S. (2008). Unsupervised segmentation of natural images via lossy data compression. *Computer Vision and Image Understanding*, *110*(2), 212-225.

Yue, X. & Zhang, H., (2019). A multi-level image thresholding approach using Otsu based on the improved invasive weed optimization algorithm. *Signal, Image and Video Processing*, 14(3), 575-582.

Zhou, M., Hong, X., Tian, Z., Dong, H., Wang, M., & Xu, K. (2014). Maximum Entropy Threshold Segmentation for Target Matching Using Speeded-Up Robust Features. *Journal of Electrical and Computer Engineering*, 1-12.

Zhou, Z., Zang, Y., Li, Y., Zhang, & Luo, X. (2013). Rice plant-hopper infestation detection and classification algorithms based on fractal dimension values and fuzzy C-means. *Mathematical and Computer Modelling*, *58*(3-4), 701-709.

B.Rajendra Prasad is a Ph.D student at the Dept. of ECE, JNTUA, A.P, India. He received his M.Tech from S.V University College of Engineering, Tirupati. His research interests include Digital Image Processing, Machine Learning, Embedded Systems.

Professor Dr.T. RamaShri is a Professor at the Dept. of ECE, S.V.U College of Engineering, Tirupati. She is a life member of IEEE, ISTE, and IETE. Her research interests include Digital Image Processing, Machine Learning, Deep Learning.

Professor Dr. K. Rama Naidu is a Professor at the Dept. of ECE at JNTUA. He received his B.Tech. Degree in ECE from JNTUA, an M.Tech. Degree in Microwave Engineering from IIT, BHU, and a Ph.D. degree in Electrical Engineering from IITK, His research interests include Channel Modelling, Resource Allocation for Wireless Relay Systems, PAPR Reduction in OFDM, Channel Estimation, and Cognitive Radios.